AIAA 81-0008R

Wing-Alone Aerodynamic Characteristics at High Angles of Attack

Robert L. Stallings Jr.* and Milton Lamb†
NASA Langley Research Center, Hampton, Va.

An experimental investigation has been conducted to determine wing-alone supersonic aerodynamic characteristics at high angles of attack. The family of wings tested had aspect ratios of 0.5-4.0 and taper ratios of 0.0-1.0. The wings were tested at angles of attack ranging from −5 to +60 deg and Mach numbers of 1.6-4.6. The aerodynamic characteristics were obtained by integrating local pressures measured over the wing surface. Presented and discussed are results showing the effects of model geometry, Mach number, and angle of attack on aerodynamic characteristics consisting of normal force, pitching moment, bending moment, longitudinal center-of-pressure locations, and lateral center-of-pressure locations.

Nomenclature

$\mathcal{R}$ = aspect ratio
b = span
C_{bm} = wing half-panel bending moment coefficient, bending moment/$[q(S/2)(b/2)]$
C_m = pitching moment coefficient, pitching moment/$(qS\bar{c})$
C_N = normal force coefficient, normal force/qS
$\bar{c}$ = mean aerodynamic chord
L = length of root chord
M = freestream Mach number
M_{NOM} = nominal freestream Mach number
q = freestream dynamic pressure
S = wing area
x = longitudinal distance measured downstream along root chord from wing apex
x_{cent} = value of x at area centroid location
x_{cp} = value of x at measured longitudinal center-of-pressure location
y = perpendicular distance from longitudinal axis of symmetry
y_{cent} = value of y at wing half-panel area centroid location
y_{cp} = value of y at lateral center-of-pressure location
α = angle of attack
Λ = leading-edge sweep angle
λ = taper ratio

Introduction

THE high-maneuverability requirements of missiles often necessitate flight at high angles of attack. At these high angles of attack, potential flow methods and linear theories have very limited applications, and the missile designer generally resorts to semiempirical methods based on wind-tunnel data for preliminary design purposes. However, there is a lack of a systematic data base of wing forces and moments as a function of aspect ratio, taper ratio, and Mach number at high angles of attack.[1] This lack of data results in part from the difficulty associated with mounting a wing without support interference at these conditions. In order to provide some of the needed high-angle-of-attack data, an experimental program was conducted at the NASA Langley Research Center using pressure models and a dog-leg sting mounting system that resulted in minimum sting interference effects. Aerodynamic forces and moments were obtained by integrating the pressure measurements. The family of wings tested had aspect ratios of 0.5-4.0 and taper ratios of 0-1.0. Angle of attack was varied from −5 to +60 deg at Mach numbers of 1.6-4.6.

Results presented and discussed are aerodynamic data consisting of normal force, pitching moment, bending moment, and longitudinal and lateral center-of-pressure locations. The results are also compared with previously published data.

Models, Instrumentation, and Test Facilities

The family of wings tested consisted of 10 models that had aspect ratios of 0.5-4.0 and taper ratios of 0.0-1.0. The configuration planforms are shown in Fig. 1 and the basic model dimensions are listed in Table 1.

Also shown in Fig. 1 is the model assembly consisting of a dog-leg sting that was designed to minimize support interference effects on the wing surface opposite the sting attach point. This surface was instrumented with approximately 60 pressure orifices with a typical layout shown in Fig. 1. Pressure measurements from these orifices were integrated over the surface area to obtain forces and moments. Since the wings were symmetrical about the longitudinal centerline, most of the pressure instrumentation was located on only half

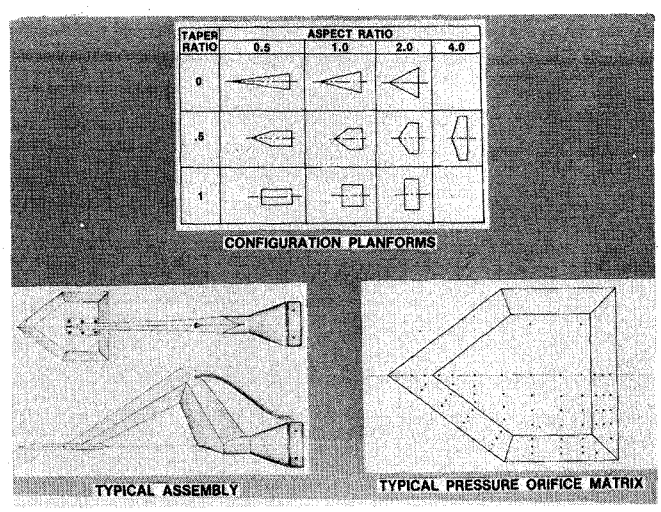

Fig. 1 Description of models and support assembly.

Presented as Paper 81-0008 at the AIAA 19th Aerospace Sciences Meeting, St. Louis, Mo., Jan. 12-15, 1981; submitted March 6, 1981; revision received Aug. 19, 1981. This paper is declared a work of the U.S. Government and therefore is in the public domain.

*Aero-Space Technologist, Supersonic Aerodynamics Branch, High-Speed Aerodynamics Division. Member AIAA.
†Aero-Space Technologist, Supersonic Aerodynamics Branch, High-Speed Aerodynamics Division.

Table 1 Model dimensions

$\mathcal{R}$	λ	L, in.	b, in.	Λ, deg	x_{cent}, in.	y_{cent}, in.
0.5	0.0	16.971	4.244	82.87	11.315	0.707
	0.5	11.314		69.44	6.915	0.943
	1.0	8.485		0.0	4.242	1.061
1.0	0.0	12.000	6.000	75.96	8.000	1.000
	0.5	8.000		53.13	4.889	1.333
	1.0	6.000		0.0	3.000	1.500
2.0	0.0	8.485	8.485	63.43	5.657	1.414
	0.5	5.657		33.69	3.457	1.886
	1.0	4.243		0.0	2.121	2.121
4.0	0.5	4.000	12.000	18.43	2.444	2.667

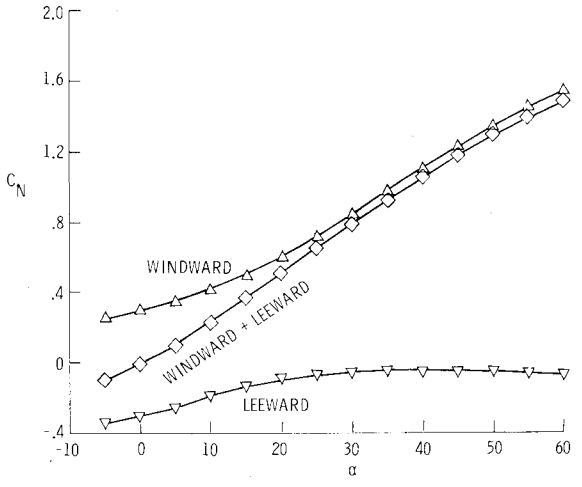

Fig. 2 Typical force data from integrated pressures, $M=2.16$, $\mathcal{R}=0.5$, $\lambda=0.5$.

a wing panel. Two orifices were located on the opposite panel to insure flow symmetry. In all tests, the sting was attached to the wing surface opposite that on which pressure measurements were being made.

All models had planform areas of 36 in.^{2}, a maximum thickness of 0.5 in., and leading edges, tips, and trailing edges consisting of sharp wedges having a total angle of 30 deg measured in a plane perpendicular to the edge.

The pressures were measured by electrical transducers connected to a pressure scanning system. A total of three scanners were used with tubing from approximately 20 orifices connected to each scanner. Four reference pressures were also connected to each scanner to provide transducer calibrations for each test point. Different reference pressures were used for the windward and leeward tests; the maximum reference pressure for each case was selected to approximately match the maximum anticipated pressure to be measured. The reference pressures and tunnel freestream pressures were measured independently by precision mercury manometers.

The tests were conducted in both the low-speed leg and high-speed leg of the Langley Unitary Plan Wind Tunnel.[2] The model angle of attack was varied from -5 to $+60$ deg for test Mach numbers ranging from 1.6-4.6. All tests were conducted at a constant freestream unit Reynolds number of 2×10^6/ft.

Data Reduction

Forces and moments were obtained by integrating the pressures over the windward and leeward surfaces. These integrated values were combined to obtain total forces and moments as illustrated in Fig. 2 for the case of normal force. Since, in some cases, the angles of attack for the windward and leeward tests were slightly different, the integrated forces and moments were evaluated at the nearest integer value of angle of attack using a second-order Lagrangian interpolation before combining the results from the two surfaces. Pitching moments were calculated about the area centroids which are given in Table 1. Bending moments were calculated about the longitudinal axis of symmetry. It should be noted that since the forces and moments were evaluated for only half a wing panel, the reference area used to determine the force and moment coefficients were half the wing planform areas, or 18 in.^{2} However, the values of C_N, C_m, and x_{cp} as presented, would also be applicable for a complete wing panel since the flow is symmetrical about the longitudinal axis of symmetry.

Results and Discussion

Before discussing in detail the results of the present tests, some indication of the validity of the results will be shown by comparisons with previously published data that were obtained using different test techniques.

Presented in Fig. 3 are comparisons of C_N, x_{cp}, and y_{cp} from the present tests with some previously published wing-alone data. The Hill data (C_N) are from force balance measurements using a sting-supported model.[3] The Falumin data (C_N and x_{cp}) were obtained using both force balance and pressure measurements.[4] The Baker data (C_N, x_{cp}, and y_{cp}) were obtained from force balance measurements using half-span wings attached to a reflection plane.[5] The results shown from Nielsen[6] are a tabulation of data that were extracted from existing wind-tunnel data including Refs. 3-5. It should be noted that most of the referenced data shown in Fig. 3 were not directly available for the indicated aspect ratio, taper ratio, or Mach number, but were determined for this comparison by a linear interpolation of the available data with respect to these variables. The comparisons shown are for a nominal Mach number of 3.

In general, results from the present tests are in good agreement with the results from the literature presented in Fig. 3 with the exception of the Baker data[5] at the larger angles of attack. This set of data is affected by flow separation on the reflection plane at the larger angles of attack, resulting in poor agreement with the other data shown. Results shown in Fig. 3 indicate the angle of attack corresponding to the onset of this separation phenomena increases with increasing aspect ratio.

Summaries of the present aerodynamic data are presented in Figs. 4 and 5 showing effects of aspect ratio, taper ratio, and Mach number. Shown in Fig. 4a is the effect of aspect ratio and taper ratio on normal force coefficient at a constant Mach number of 2.16. Shown on the left side of the figure is the effect of aspect ratio for a taper ratio of 0.5 and on the right is the effect of taper ratio for an aspect ratio of 1. In general, increasing aspect ratio results in an increase in C_N for the test range of aspect ratio. As shown on the right figure, increasing the taper ratio from 0 to 0.5 results in an increase in C_N; however, C_N remains essentially constant when increasing the taper ratio from 0.5 to 1.

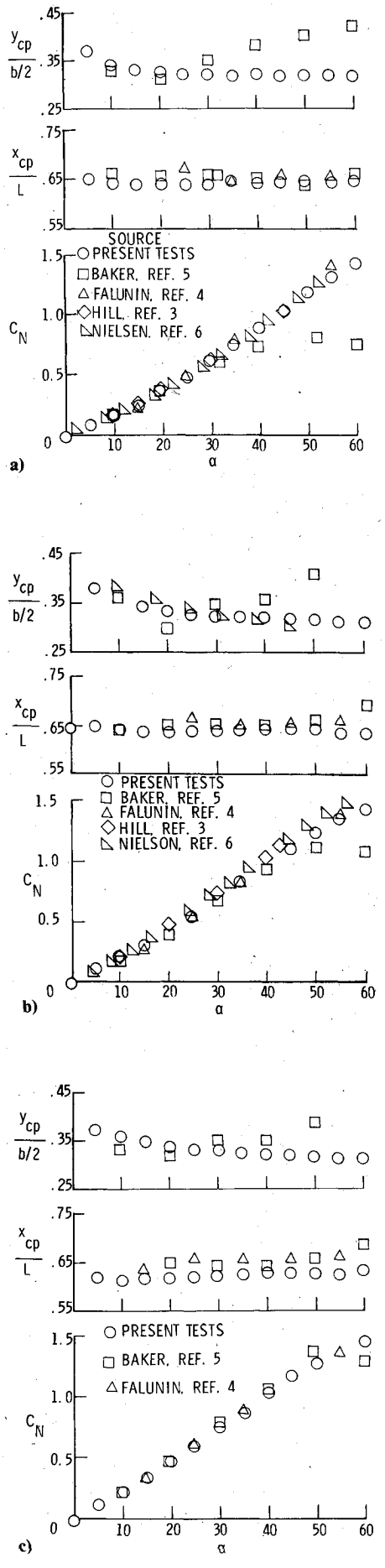

Fig. 3 Comparison of present data with previously published data, $M_{NOM} = 3$, $\lambda = 0$: a) $AR = 0.5$; b) $AR = 1.0$; c) $AR = 2.0$.

Shown in Fig. 4b is the effect of model geometry on the pitching moment coefficient with aspect ratio effects again shown on the left and taper ratio effects shown on the right. For these tests, the moment center for pitching moments is the area centroid and the coefficients are based on a reference length equal to the mean aerodynamic chord. For all but the maximum test angles of attack, increasing either aspect ratio or taper ratio resulted in large increases in pitching moment coefficient with the maximum values occurring at the approximate angle of attack at which freestream pitot pressure was first measured on the windward surface of the wing apex region. This measurement of freestream pitot pressure implies that the stagnation point or stagnation region has moved from the wing leading edge onto the windward wing surface. With further increases in angle of attack, the stagnation point moves toward the area centroid resulting in a decrease in C_m. At the maximum test angle of 60 deg, there is no effect of either aspect ratio or taper ratio on C_m.

Shown in Fig. 4c is the effect of model geometry on bending moment coefficient. These coefficients are based on a moment taken about the longitudinal centerline and a reference length equal to the wing semispan. The variation of bending moment coefficient with aspect ratio is very similar to the variation of C_N with aspect ratio, indicating that the lateral center-of-pressure location nondimensionalized by the semispan is about the same for these four models. However, the increase of C_{bm} with increasing taper ratio is considerably greater than the increase of C_N with taper ratio shown previously, implying that the nondimensional lateral center-of-pressure location for these three models moves outboard with increasing taper ratio. Such variations in the center-of-pressure locations were measured and will be shown subsequently.

Shown in Fig. 4d is the effect of model geometry on the longitudinal center-of-pressure location (x_{cp}) nondimensionalized by centerline length. The solid symbols in both figures represent the values of x/L corresponding to the wing area centroids. For the four $\lambda = 0.5$ models (left figure) the area centroids are located at approximately 61% of the centerline length downstream of the apex. For the three $AR = 1.0$ wings (right figure) the area centroid locations vary from approximately 67% of the centerline length for $\lambda = 0$ to 50% for $\lambda = 1.0$. Except for the maximum test angles of attack, increasing aspect ratio results in a forward movement of the nondimensional center-of-pressure location. At the maximum test angle of attack, the nondimensional center-of-pressure locations for all four wings having a taper ratio of 0.5 are located at $x/L \approx 0.55$. This center-of-pressure location is rapidly approached once the stagnation point moves onto the windward wing surface and approaches the area centroid. The right-hand side of Fig. 4d shows that increasing taper ratio for $AR = 1$ results in a forward movement of the center-of-pressure locations. These results also show that the center-of-pressure location approaches the area centroids at the maximum test angle of attack.

Shown in Fig. 4e is the effect of model geometry on the lateral center-of-pressure location (y_{cp}) nondimensionalized by wing semispan ($b/2$). The lateral location of the area centroids are indicated by the solid symbols. The data presented in the left figure for constant λ show that the nondimensional lateral center-of-pressure location is relatively insensitive to aspect ratio. The data presented in the right figure for constant aspect ratio show that the nondimensional lateral center-of-pressure location moves outboard with increasing taper ratio. These effects of aspect ratio and taper ratio on lateral center-of-pressure locations are consistent with the finding previously discussed for the bending moment results. Both sets of data presented in Fig. 4e show that the centers of pressure approach the area centroids at the larger angles of attack.

Shown in Figs. 5a and 5b is the effect of Mach number on C_N and C_m for the wing with $AR = 1.0$ and $\lambda = 0.5$. In general,

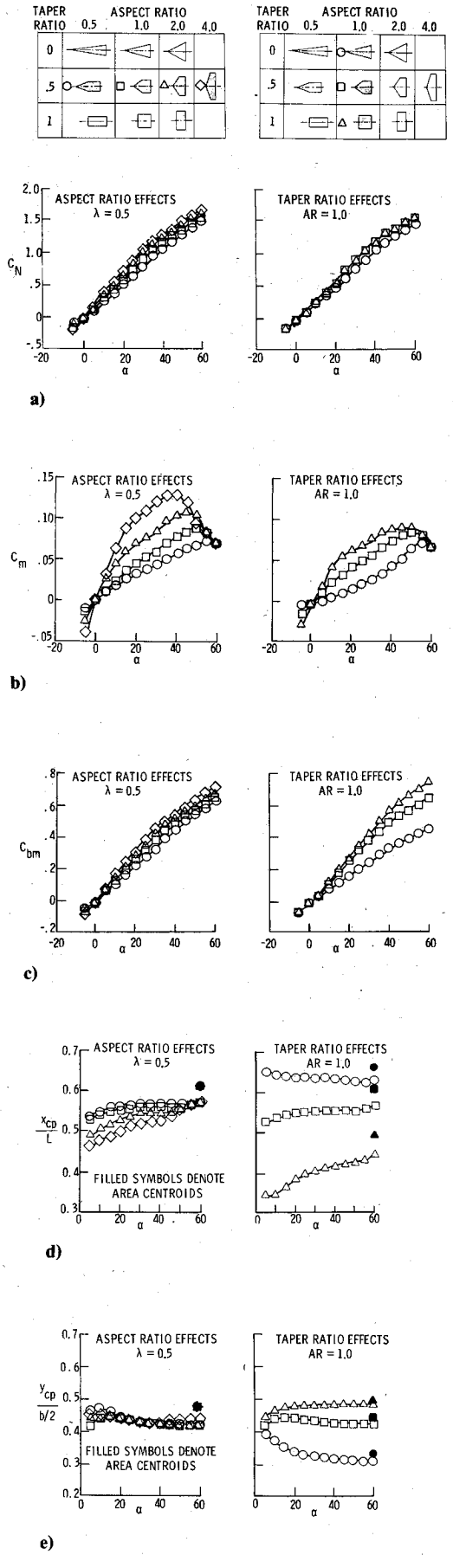

Fig. 4 Effect of model geometry on measured aerodynamic characteristics, $M = 2.16$: a) normal force coefficient; b) pitching moment; c) bending moment; d) longitudinal center of pressure; e) lateral center of pressure.

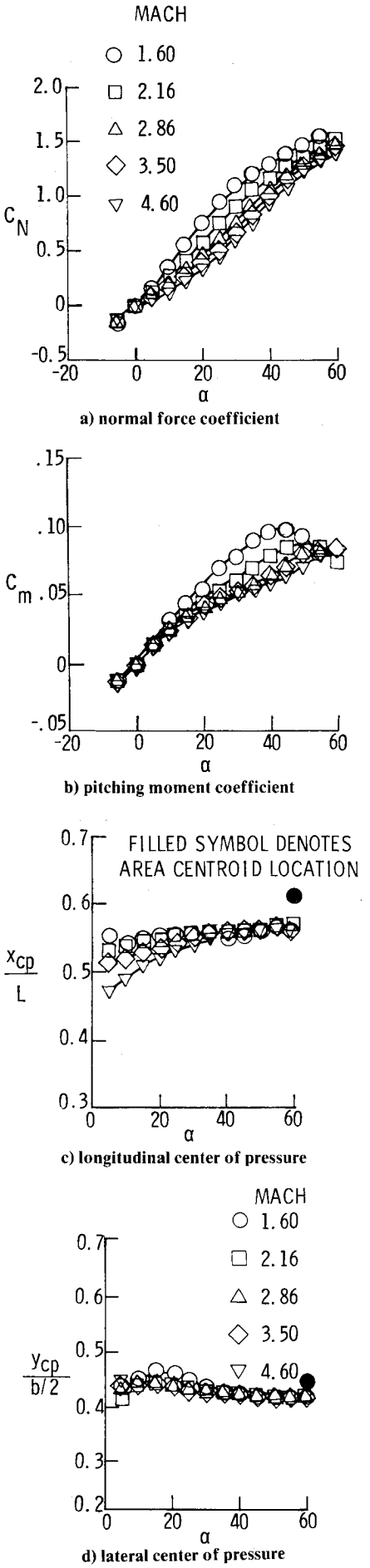

Fig. 5 Effect of Mach number on measured aerodynamic characteristics, $AR = 1.0$, $\lambda = 0.5$.

increasing Mach number results in a decrease in both C_N and C_m with the exception of C_m at the maximum test angles which is relatively unaffected by Mach number. Also, increasing Mach number results in an increase in the angle of attack at which peak C_m is measured as a result of the higher angles associated with shock detachment.

Shown in Figs. 5c and 5d is the effect of Mach number on x_{cp}/L and $y_{cp}/(b/2)$ also for the wing with $AR = 1.0$ and taper ratio = 0.5. For $\alpha > 30$ deg, the results show that for the test range of Mach numbers, both x_{cp}/L and $y_{cp}/(b/2)$ are insensitive to Mach number. For $\alpha < 30$ deg, x_{cp}/L decreases with increasing Mach number for the complete test Mach number range and $y_{cp}/(b/2)$ decreases with increasing Mach number for $1.6 \leq M \leq 2.86$. Further increases in Mach number have no effect on $y_{cp}/(b/2)$.

Conclusion

An experimental investigation has been conducted to determine wing-alone supersonic aerodynamic characteristics at high angles of attack. The family of wings tested had aspect ratios of 0.5-4.0 and taper ratios of 0.0-1.0. The wings were tested at angles of attack from -5 to $+60$ deg and Mach numbers of 1.6-4.6. The aerodynamic characteristics were obtained by integrating pressure measurements over the surfaces of the wings. Results from these tests lead to the following conclusions:

1) Longitudinal and lateral center-of-pressure locations approached the area centroids at the maximum test angles of attack.

2) For angles of attack greater than 30 deg, longitudinal and lateral center-of-pressure locations were unaffected by Mach number.

3) Peak pitching moment coefficients were measured at the approximate angle of attack at which freestream pitot pressure was first measured on the windward surface in the wing apex region.

4) Increasing aspect ratio resulted in a general increase in normal force coefficient (C_N). Increasing taper ratio (λ) from 0 to 0.5 resulted in an increase in C_N but further increases in λ had little effect on C_N.

References

[1] Nielsen, J.N., "Nonlinearities in Missile Aerodynamics," AIAA Paper 78-20, Jan. 1978.

[2] *Manual for Users of the Unitary Plan Wind Tunnel Facilities of the National Advisory Committee for Aeronautics,* NASA, 1956.

[3] Hill, W.A. Jr., "Experimental Lift of Low-Aspect-Ratio Triangular Wings at Large Angles of Attack and Supersonic Speeds," NACA RM A57I17, 1957.

[4] Falunin, M.P., Ul'yanov, G.S., Makshin, A.A., and Mosin, A.F., "Supersonic Aerodynamic Characteristics of Delta Wings at High Angles of Attack," *Fluid Dynamics,* Vol. 3, Sept.-Oct. 1968, pp. 105-108.

[5] Baker, W.B. Jr., "Static Aerodynamic Characteristics of a Series of Generalized Slender Bodies With and Without Fins at Mach Numbers From 0.6 to 3.0 and Angles of Attack from 0 to 180 Degrees," Vols. I and II, AEDC-TR-75-124 (Rev.) and AEDC-TR-75-124, May 1976.

[6] Nielsen, J.N., Hemsch, M.J., and Smith, C.A., "A Preliminary Method for Calculating the Aerodynamic Characteristics of Cruciform Missiles to High Angles of Attack Including Effects of Roll Angle and Control Deflections," ONR-CR-215-226-4F, Nov. 1, 1977 (available from DTIC as AD A054 349).